JPET Fast Forward. Published on October 14, 2010 as DOI:10.1124/jpet.110.172668

Iron-induced cardiac damage: role of apoptosis and deferasirox intervention

Yeling Wang, Miaozong Wu, Rabaa Al-Rousan, Hua Liu, Jacqueline Fannin, Satyanarayana Paturi, Ravi Kumar Arvapalli, Anjaiah Katta, Sunil K. Kakarla, Kevin M. Rice, William E. Triest, and Eric R. Blough

Center for Diagnostic Nanosystems, Marshall University (Y.W., M.W., R.A., H.L., J.F., S.P., R.K.A., A.K., S.K.K., K.M.R., and E.R.B), Department of Biological Sciences, Marshall University (M.W., S.P., R.K.A., K.M.R., and E.R.B), Department of Exercise Science, Sport and Recreation, Marshall University (M.W., K.M.R., and E.R.B), Department of Pharmacology, Physiology and Toxicology, Marshall University, Huntington, West Virginia, United States of America (R.A., J.F., A.K., S.K.K., and E.R.B), The First Hospital, Jilin University, Jilin, China (Y.W.), Department of Physiology and Pharmacology, Southeast University, Nanjing, China (H.L.). Huntington VA Medical Center (W.E.T).

Copyright 2010 by the American Society for Pharmacology and Experimental Therapeutics.

Running Title: Iron-induced cardiac apoptosis and Deferasirox intervention.

Author for correspondence:

Eric Blough, Ph.D.

Center for Diagnostic Nanosystems

241N Byrd Biotechnology Building, Marshall University

1 John Marshall Drive, Huntington, WV 25755-1090

Phone: (304) 696-2708; Fax: (304) 696-7136

E-mail: blough@marshall.edu

Counts :

No. of text pages: 24

No. of tables: 0

No. of figures: 6

No. of references: 42

No. of words in Abstract: 219

No. of words in Introduction: 582

No. of words in Discussion: 1551

Abbreviations: DFR, deferasirox, ExjadeR, ICL670; FHC, ferritin heavy chain; FLC, ferritin light chain; GAPDH, glyceraldehyde 3-phosphate dehydrogenase; HO, reactive hydroxyl radicals; ICP-AES, inductively coupled plasma-atomic emission spectroscopy; IO, iron loading; IRE, iron-responsive element; IRP, iron-responsive element-binding protein; ROS, reactive oxygen species; T-PER, Tissue Protein Extraction Reagent; TUNEL, terminal deoxyribonucleotide transferase-mediated dUTP nick end-labeling assay.

Recommended section: Cardiovascular

Abstract

Excess cardiac iron levels are associated with cardiac damage and can result in increased morbidity and mortality. Here we hypothesize that elevations in tissue iron can activate caspase-dependent signaling which lead to increased cardiac apoptosis and fibrosis, and that these alterations can be attenuated by iron chelation. Using iron-overloaded gerbil model, we show that increased cardiac iron is associated with reduced activation of Akt (Ser473 and Thr308), diminished phosphorylation of the pro-apoptotic regulator Bad (Ser136), and an increased Bax / Bcl-2 ratio. These alterations were coupled with increased activation of the downstream caspase-9 (40/38- and 17-kDa fragments) and apoptosis executioner caspase-3 (19- and 17-kDa fragments), which were accompanied by evidence of elevated cytoskeletal alpha-fodrin cleavage (150- and 120-kDa fragments), discontinuity of myocardial membrane dystrophin immunoreactivity, increases in the number of TUNEL positive cells (nucleic DNA fragmentation) and cardiac fibrosis. Importantly, we demonstrate that administration of deferasirox, a tridentate iron chelator, is associated with diminished tissue iron deposition, attenuated activation of caspases, reduced alpha-fodrin cleavage, improved membrane integrity, decreased TUNEL reactivity and an attenuation of cardiac fibrosis. These results suggest that the activation of caspase-dependent signaling may play a role in the development of iron-induced cardiac apoptosis and fibrosis, and deferasirox, via a reduction in cardiac tissue iron levels, may be useful for decreasing the extent of iron-induced cardiac damage.

Introduction

Excess tissue iron content due to iron overload or accumulation is estimated to affect up to one hundred million worldwide and is often seen in individuals with hereditary haemochromatosis and in those who require frequent blood transfusions, such as individuals afflicted with thalassemia, sickle cell disease, and myelodysplastic syndrome (Burke et al., 2002; Abetz et al., 2006). Excess tissue iron accumulation is toxic and can lead to heart failure which is the major cause of death following protracted iron overload (Borgna-Pignatti et al., 2005; Kohgo et al., 2008). Although the causes of cardiomyopathy following iron overload are not fully understood, it has been suggested that iron overload is associated with increases in myocardial apoptosis and the development of fibrosis (Whittaker et al., 1996; Oudit et al., 2004; Arvapalli et al., 2010).

The factors regulating apoptosis are complicated however several studies have posited that caspase-3 plays a central role in the execution-phase of cell apoptosis (Janicke et al., 1998; Porter and Janicke, 1999). The activation of caspase-3 is governed by a group of signaling cascade, among which the interaction of the anti-apoptotic Bcl-2 and the pro-apoptotic Bax proteins plays a critical role. Indeed, recent data has demonstrated that Bcl-2 is capable of forming a heterodimer with Bax thereby preventing Bax homodimerization, the release of mitochondria cytochrome C, activation of protease caspase-9 and subsequent caspase-3 (Gross et al., 1998; Narita et al., 1998; Murphy et al., 2000). In addition to Bax/ Bcl-2 signaling, activation of caspase-mediated proteolytic cascade can also be regulated by another pro-apoptotic factor Bad. The Bad can affect the binding of Bax to Bcl-2 through its ability to bind to Bcl-2 (Yang et al., 1995). It is thought that the ability of Bad to bind to Bcl-2 is abrogated when Bad becomes phosphorylated at Ser136 by Akt / protein kinase B, a serine/threonine-specific protein kinase that is involved in regulating cell survival (Zha et al., 1996; Datta et al., 1997; Wu et al., 2010c). Whether iron overload affects the regulation of these caspase-mediated proteolytic cascades is currently unclear.

The initial treatment for the accumulation of excess iron is typically pharmacological intervention with deferoxamine or deferiprone. While effective, treatment compliance is frequently compromised as the administration of these compounds is often burdensome or associated with serious side effects

(Neufeld, 2006). Work from the last few years has suggested that once daily treatment with deferasirox (Exjade^{R}, ICL670. $C_{21}H_{15}N_3O_4$), an orally administered tridentate iron chelator, may be effective for the treatment of the treatment of iron overload (Neufeld, 2006; Al-Rousan et al., 2009; Arvapalli et al., 2010; Pennell et al., 2010). Although initial findings regarding the use of deferasirox have demonstrated effectiveness in removing cardiac iron in animals and humans, whether this agent is capable of diminishing iron-associated increases in cardiomyocyte apoptosis and fibrosis has not been investigated.

Previous studies from our laboratory using the Mongolian gerbil model have demonstrated that deferasirox treatment is capable of reducing cardiac iron content following iron overload (Al-Rousan et al., 2009). Further using a subset of animals and tissues from this project (Al-Rousan et al., 2009), here we hypothesize that excess tissue iron can activate caspase-dependent signaling which lead to increased cardiac apoptosis and fibrosis, and these alterations can be attenuated by iron chelation. Our findings demonstrate that iron overload in the heart is associated with increased activation of caspase-3, elevated alpha-fodrin cleavage and discontinuity of myocardial membrane, along with increased nucleic DNA fragmentation and cardiac fibrosis, and deferasirox treatment is effective in attenuating iron-overload associated cardiac damage.

Materials and Methods

Materials

Primary antibodies against caspase-3 (#9662), caspase-9 (#9506), alpha-Fodrin (#2122), Bcl-2 (#2870S), Bax (#2772), Akt (#9272), phospho-Akt (Thr308) (pAkt-Thr308, #9275S), phospho-Akt (Ser473) (pAkt-Ser473, #9271), Bad (#9239s), phospho-Bad (Ser136)(pBad, #9295s), glyceraldehyde 3-phosphate dehydrogenase (GAPDH, #2118), and rabbit secondary antibodies (#7074, anti-rabbit) were purchased from Cell Signaling Technology (Beverly, MA). Ferritin heavy chain (H-53) (#25617) antibodies were from Santa Cruz Biotechnology (Santa Cruz, CA). Ferritin light chain (#FERL14-A) antibodies were procured from Alpha Diagnostic International (San Antonio, TX). The dystrophin antibody (#NCLDYS2) was from Novocastra Vector Laboratories (Burlingame, CA) while the *in situ* cell death detection kit was from Roche Diagnostics (Mannheim, Germany). VECTASHIELD HardSet Mounting Medium with DAPI was from Vector Laboratories (Burlingame, CA). Picro-sirius red was from POLY SCIENTIFIC (Bay Shore, NY). Pierce Tissue Protein Extraction Reagent (T-PER) and Pierce 660nm protein assay reagent (#22660) were from Thermo Fisher Scientific Inc (Rockford, IL). PAGEr Gold Precast gels (10% and 15%) were from Lonza (Rockland, ME) while ECL Western Blotting reagent (#RPN 2106) and ECL Advance Western Blotting Detection Kit (#RPN 2135) were from GE Healthcare Bio-Sciences Corp (Piscataway, NJ). Dual Color molecular weight markers were from BioRad (Hercules, CA). Protease inhibitors (#P8340), phosphatase inhibitors (#P5726), SDS-loading buffer, iron stain kit (HT20-1), poly-lysine and iron dextran were purchased from Sigma (Sigma-Aldrich, Inc., St. Louis, MO, USA). RAPID Stain was from G-Biosciences (St. Louis, MO, USA). Deferasirox was provided by Novartis Pharmaceuticals (East Hanover, NJ). All other chemicals were purchased from Sigma (St. Louis, MO).

Animals, iron overload, deferasirox treatment and tissue collection

Animal care and procedures were conducted in accordance with the Animal Use Review Board of Marshall University using the criteria outlined by the American Association of Laboratory Animal Care

as proclaimed in the Animal Welfare Act (PL89-544, PL91-979, and PL94-279). Adult male Mongolian gerbils (*Meriones unguiculatus*) were obtained from Charles River Laboratories (Wilmington, MA) and housed four per cage. Housing conditions consisted of a 12H:12H dark-light cycle with temperature maintained at 22 ± 2 °C. Animals were provided food and water *ad libitum*. Gerbils were divided into five groups as follows: iron overloaded for 10 weeks and sacrificed immediately after iron loading (IO), 3-months treated with deferasirox (IO-DFR) or vehicle peanut butter (IO-3m) following 10-weeks of iron loading, age-matched control for the 10-week iron loading protocol (C) and age-matched control for the 3-month treated animals (C-3m). As detailed previously (Al-Rousan et al., 2009), iron treated animals received 15 subcutaneous injections of iron dextran at a dose of 100 mg/kg, while deferasirox was given orally in a single daily dosage of 100 mg/kg after suspension in plain peanut butter. Hearts were removed from anesthetized animals, sliced into three sections, each frozen in liquid nitrogen, and stored at − 80°C. The middle section was used for histological analysis while the apex and base were used for protein extraction as detailed previously (Wu et al., 2009a; Wu et al., 2009b).

TUNEL assay

The middle section of hearts were serially sectioned (8 μm) using an IEC Minotome cryostat and collected on poly-lysine coated slides. DNA fragmentation was detected by using a terminal deoxyribonucleotide transferase-mediated dUTP nick end-labeling (TUNEL) assay. TUNEL, dystrophin and DAPI triple-staining were performed as described previously (Wu et al., 2009b; Arvapalli et al., 2010; Kakarla et al., 2010).

Measurement of collagen content

Picro-sirius red staining was used to measure interstitial collagen on heart sections as described elsewhere (Dolber and Spach, 1987). Briefly, tissue sections fixed with 95% alcohol for 1 minute, washed three times with tap water and then stained with hematoxylin for 8 minutes and picrosirius red for 20 minutes. After dehydration sections and mounting, collagen content was determined from fifteen

randomly selected regions from each tissue section at 40X magnification using an Olympus BX51 microscope. Collagen area was measured using ImageJ program as outlined previously (Wu et al., 2009b).

Perls iron stainning

Tissue iron distribution was determined via a Perls iron staining according to the manufacturer's protocol. The area of iron deposition was quantified using Image J program.

Immunoblotting analysis

Tissue protein were extracted via homogenization in T-PER buffer containing protease and phosphatase inhibitors as detailed previously (Wu et al., 2009a; Wu et al., 2009b; Wu et al., 2010b). Protein concentration of homogenates was determined via the Bradford method. Forty micrograms of protein were boiled in SDS-loading buffer and separated on 10% or 15% SDS-PAGE gels before being transferred to nitrocellulose membranes as described elsewhere (Wu et al., 2009a; Wu et al., 2009b; Arvapalli et al., 2010; Wu et al., 2010b). Gels were stained with RAPID protein reagent to confirm equal protein loading and the transfer efficiency of proteins onto membrane. Antigens of interest were visualized following incubation of membranes with specific antibodies and development with ECL reagent. Target protein levels were quantified by AlphaEaseFC image analysis software and normalized to the amount of GAPDH.

Data analysis:

The results are presented as mean ± SE. Data were analyzed by using Sigma Stat 3.5 software. The effects of iron and the role of deferasirox were evaluated by ANOVA followed by the Student-Newman-Keuls test for multiple-comparison testing. Values of $P < 0.05$ were considered to be statistically significant.

Results

Deferasirox treatment reduces cardiac iron deposition

Gerbils were divided into five groups as follows: iron overloaded for 10 weeks and sacrificed immediately after iron loading (IO), 3-months treated with deferasirox (IO-DFR) or vehicle peanut butter (IO-3m) following 10-weeks of iron loading, age-matched control for the 10-week iron loading protocol (C) and age-matched control for the 3-month treated animals (C-3m). As detailed previously (Al-Rousan et al., 2009), inductively coupled plasma-atomic emission spectroscopy (ICP-AES) demonstrated that cardiac iron content was 10.4 fold higher following 10 weeks of iron overload (IO) and 7.4 fold higher after 3 months of follow up (IO-3m). Once daily treatment with deferasirox significantly decreased overload-induced cardiac iron levels (Al-Rousan et al., 2009). Perl's staining of cardiac sections was used to expand upon these findings and demonstrated that iron was deposited both within and outside cardiomyocytes of the iron-overloaded gerbil heart (Figure 1A). Consistent with our ICP-AES data, iron overload significantly increased the area of cardiac tissue that reacted positively for iron ($P < 0.05$). This finding persisted in the 3-month follow up animals ($P < 0.05$) but was significantly reduced following deferasirox treatment ($P < 0.05$; Figure 1A). Supporting our findings of increased tissue iron, iron overload significantly increased the amount of ferritin heavy and light chain, two key regulators of iron metabolism and storage (Kohgo et al., 2008; Arvapalli et al., 2010) both post loading and after 3-months of follow up ($P < 0.05$). Consistent with our measurement of tissue iron, deferasirox treatment decreased the abundance of ferritin heavy and light chain ($P < 0.05$; Figure 1B).

Deferasirox diminishes iron overload-induced myocardial fibrosis

To examine the potential effects of increased tissue iron on cardiac fibrosis, Pico-sirius red staining was used to semi-quantitatively assess collagen accumulation. Iron overload significantly increased collagen deposition whether examined immediately following the loading period or after the 3-

month follow up period ($P < 0.05$; Figure 2). Compared to age-matched controls, deferasirox treatment significantly decreased cardiac collagen accumulation (- 54%, $P< 0.05$; Figure 2).

Deferasirox decreases iron overload-induced cardiomyocyte nucleic DNA fragmentation

To investigate the possibility that tissue iron accumulation was associated with an increase in cardiomyocyte apoptosis, we examined the number of nuclei staining positively for DNA fragmentation using terminal deoxyribonucleotide transferase-mediated dUTP nick end-labeling (TUNEL) staining. Compared with age-matched controls, the number of TUNEL positive nuclei was significantly increased both after iron overload and remained elevated through 3-months of follow up ($P < 0.05$; Figure 3). Deferasirox treatment was associated with a significant decrease in the number of TUNEL reactive cells (- 77%, $P< 0.05$; Figure 3).

Deferasirox decreases iron overload-induced activation of caspases

Caspase-3 is a critical executioner of apoptosis (Janicke et al., 1998; Porter and Janicke, 1999). Compared to age-matched controls, iron overload increased the amount of the cleaved (activated) caspase-3 (19 kDa and 17 kDa fragments) immediately after- and at 3-months post iron overload ($P < 0.05$; Figure 4A). This finding was attenuated with deferasirox treatment as the amount of caspase cleavage was decreased by 51% and 53% for the 19 kDa and 17 kDa fragments, respectively ($P < 0.05$; Figure 4A).

To confirm our findings of increased caspase-3 activation with iron overload we next examined the activity of caspase-9 which is thought to be an upstream regulator of caspase-3 (Janicke et al., 1998). Similar to caspase-3 data, the amount of cleaved (active) caspase-9 (40/38- and 17-kDa) was significantly increased following iron overload and in the 3-months follow up animals ($P < 0.05$; Figure 4B). Compared to age-matched controls, deferasirox treatment significantly decreased the iron overload-

induced activation of caspase-9 by 51% and 54% for the 40/38 kDa and 17 kDa fragments, respectively ($P < 0.05$; Figure 4B).

As a next step we investigated if iron-induced caspase-3 activation was associated with increased cleavage of alpha-fodrin. This molecule was chosen on the basis of previous reports suggesting that alpha-fodrin is a substrate of caspase-3 and because of its critical role in stabilizing the cell membrane (Martin et al., 1995; Janicke et al., 1998; Kakarla et al., 2010). Consistent with our findings of increased caspase-3 activation, the amount of cleaved alpha-fodrin (150- and 120-kDa) was significantly increased following iron overloaded and after 3-months of follow up ($P < 0.05$; Figure 4C). Deferasirox treatment decreased iron overload-induced fragmentation of alpha-fodrin by 56% and 52% for the 150- and 120-kDa fragments, respectively ($P < 0.05$; Figure 4C).

Because the cleavage of alpha-fodrin has been linked to increases in membrane blebbing and the development of apoptosis (Martin et al., 1995; Janicke et al., 1998) we examined whether increased alpha-fodrin fragmentation was associated with alterations in dystrophin localization. Immunohistochemical staining demonstrated a discontinuity of myocardial membrane dystrophin immunoreactivity following iron overload and in the 3-month follow up animals while tissue sections obtained from deferasirox treated animals tended to more closely resemble those from age-matched and non-iron overloaded control animals (Figure 4D).

Deferasirox prevents iron overload–induced alterations in caspase-activation signaling

The expression of Bax, a pro-apoptotic protein critical for caspase-9 activation (Gross et al., 1998), was not different between groups ($P = 0.10$; Figure 5A), while the expression of the anti-apoptotic Bcl-2 protein (Murphy et al., 2000; Wu et al., 2009b), was decreased in the animals that had been subjected to 10 weeks of iron-overload. Deferasirox treatment increased the amount of Bcl-2 compared to that observed in age-matched IO control animals (+105%, $P< 0.05$; Figure 5A). The ratio of Bax / Bcl-2, a predictive marker of mitochondria-mediated caspase-9 activation (Korsmeyer et al., 1993), was increased in animals following 10-weeks of iron overload, while deferasirox treatment decreased the Bax

/ Bcl-2 ratio compared to that observed in age-matched iron overload control animals (- 56%, *P< 0.05*; Figure 5A).

The expression of Bad, another pro-apoptotic protein that promotes cell death by disturbing the inhibitory effects of Bcl-2 on Bax (Yang et al., 1995), was not different between groups (P = 0.17). However, phosphorylation of Bad at Ser136 which acts to inhibit the apoptotic activity of this protein was decreased following iron overload and in the 3-month follow up animals (*P < 0.05*). Deferasirox treatment significantly increased Bad (Ser136) phosphorylation compared to that of age-matched iron overload animals (*P < 0.05*; Figure 5B).

The phosphorylation of Bad at Ser136 is thought to be mediated by Akt, a kinase that functions to promote cell survival and prevent apoptosis (Zha et al., 1996; Datta et al., 1997; Wu et al., 2009b). The phosphorylation / activation of Akt at both Ser473 and Thr308 were decreased following iron overload and in the 3-months follow up animals (*P < 0.05*), while deferasirox treatment significantly increased phosphorylation of Akt to levels comparable to that seen in the age-matched iron overload animals (*P < 0.05*; Figure 5C).

Discussion

Excess tissue iron levels are toxic and can lead to myocardial injury and heart failure which is one of major causes of death in those afflicted with iron overload (Borgna-Pignatti et al., 2005; Kohgo et al., 2008). Previous work from our laboratory using the iron overloaded Mongolian gerbil has demonstrated that deferasirox is effective in reducing cardiac iron content (Al-Rousan et al., 2009). Extending upon this study, here we demonstrate that increased cardiac iron is associated with increased apoptosis and fibrosis, a finding that appears to persist over time as these alterations were also found in animals that had undergone iron loading and then analyzed 3-months later. Importantly, our data also demonstrate that deferasirox administration is effective in attenuating iron overload associated cardiac apoptosis and fibrosis.

Increases in cardiac fibrosis and apoptosis have been implicated in the pathological remodeling of the heart and have been shown to be involved in the progression to heart failure (Burlew and Weber, 2002; Gurtl et al., 2009). Using picro-sirius red staining to examine collagen deposition, we demonstrate that iron overload is associated with increased cardiac interstitial fibrosis and that the extent of fibrosis is decreased with deferasirox treatment (Figure 2). Increases in cardiac apoptosis are thought to be associated with increased cleavage of cytoskeletal protein alpha-fodrin, loss of plasma membrane integrity and increased DNA fragmentation (Majno and Joris, 1995; Martin et al., 1995; Janicke et al., 1998; Zhang and Xu, 2000; Fadeel, 2004; Takada et al., 2004). Confirming this possibility, we found an increased number of cardiac myocytes exhibiting DNA strand breaks (TUNEL positive; Figure 3), increased alpha-fodrin cleavage (Figure 4C) and discontinuity in cardiomyocyte membrane immunoreactivity for dystrophin (Figure 4D) with iron overload. Importantly, we also found that each of these alterations was attenuated by deferasirox treatment. In our previous study we have demonstrated 10 weeks of iron overload increased cardiac iron content as determined by ICP-AES (Al-Rousan et al., 2009). As an extension of that study, here we examined how iron overload affects the spatial deposition of iron in myocardium. Consistent with our aforementioned study, here we found evidence of increased iron deposition after 10-weeks of iron overload, an observation that remains present even after 3 months of

follow up. As expected, deferasirox treatment was associated with reduced iron deposition and decreased expression of ferritin heavy and light chain molecules (Figure 1A and 1B). More importantly, it is noteworthy that regions of iron deposition appeared to be spatially and quantitatively associated with areas of cellular apoptosis and fibrosis (Figures 1A, 2 and 3), a finding that is consistent with the possibility that excess iron can lead to cardiac damage.

To further our understanding of how iron overload induces apoptosis, we investigated the regulation of caspase-3. As a critical executioner of apoptosis (Janicke et al., 1998; Porter and Janicke, 1999), caspase-3 was activated after iron overload at the 3-month follow up time point (Figure 4A). This activation was associated increased activation of its upstream protease, caspase-9 (Figure 4B). To verify the functionality of caspase-3 activation, we also examined whether elevations in tissue iron were associated with the increased cleavage of alpha-fodrin, a primary target of caspase-3 that has been implicated in maintenance of normal membrane structure and supporting cell surface protein function (Martin et al., 1995; Janicke et al., 1998; Kakarla et al., 2010). We demonstrated that the 150 kDa and 120 kDa fragments of cleaved alpha-fodrin were significantly increased in animals after 10-weeks of iron overload and in the 3-month following up animals. Importantly, these iron overload-associated increases in alpha-fodrin cleavage were significantly reduced with deferasirox treatment (Figure 4C). To investigate whether the fragmentation of alpha-fodrin may affect cardiomyocyte membrane integrity we next examined the spatial distribution of dystrophin, a critical transmembrane protein (Ervasti and Campbell, 1993; Wu et al., 2009b; Kakarla et al., 2010). Interestingly, tissue sections obtained from the hearts of the iron overloaded and 3-month follow up groups both exhibited discontinuity of dystrophin immunoreactivity, a finding that was substantially diminished following deferasirox treatment (Figure 4D). Taken together, these results are consistent with the notion that iron overload is associated with activation of caspase signaling, cleavage of alpha-fodrin and disruption of cardiomyocyte membrane integrity (Figure 6).

Among the signaling molecules that have been thought to be involved in the activation of caspase-9, Bax and its regulatory partners play a critical role. Upon apoptotic stimulation, Bax stimulates

the release of mitochondrial cytochrome C which in turn is thought to activate the protease activity of caspase-9 (Korsmeyer et al., 1993; Gross et al., 1998; Narita et al., 1998; Murphy et al., 2000). It is postulated that the ratio of Bax / Bcl-2 proteins plays a critical role in regulating cellular apoptosis with cell death being favored as the balance shifts toward Bax (Korsmeyer et al., 1993; Murphy et al., 2000). Here we found that iron overload was associated with a reduction in the amount of Bcl-2 protein, resulting in a significant increase of Bax / Bcl-2 ratio (Figure 5A). As expected from our caspase data, deferasirox treatment was associated with increases in the amount of Bcl-2 expression and hence a decreased Bax / Bcl-2 ratio compared to that observed in age-matched iron overload animals (Figure 5A). These data suggest that excess tissue iron has an adverse effect on Bcl-2 expression and that deferasirox-associated reductions in caspase activation and cellular apoptosis might be related to improvements in the Bcl-2 / Bax ratio. This possibility is supported by reports in the literature as other studies, performed in vitro, have shown that elevated iron can reduce Bcl-2 expression without affecting Bax levels (Carlini et al., 2006; Kooncumchoo et al., 2006). Whether the reduction in Bcl-2 protein observed under conditions of elevated iron are due to transcriptional changes or protein degradation is currently unclear and will require further study.

It is well documented that the pro-apoptotic factor Bad can affect the binding of Bax to Bcl-2 through its ability to bind to Bcl-2 (Yang et al., 1995). It is thought that the ability of Bad to bind to Bcl-2 is abrogated when Bad becomes phosphorylated at Ser136 by Akt / protein kinase B, a serine/threonine-specific protein kinase that is involved in regulating cell survival (Zha et al., 1996; Datta et al., 1997; Wu et al., 2010c). Here we demonstrate that the degree of Bad phosphorylation (Ser136) was decreased by iron overload, even through the expression of Bad was not changed (Figure 5B). As predicted, this reduction in Bad phosphorylation was found to be associated with reduced phosphorylation / activation of Akt (Thr308 and Ser473) (Figure 5C). Consistent with the alteration of caspase activation and cellular apoptosis, deferasirox treatment restored this iron-induced reduction in Akt phosphorylation. Importantly, this treatment-related increase in phosphorylated Akt was associated with increased phosphorylation of Bad (Figure 5C). Taken together, these data suggest that Akt / Bad signaling may participate in regulation

of excess tissue iron-induced caspase activation and cellular apoptosis and that deferasirox may act to diminish the degree of apoptosis, at least in part, by its ability to improve Akt signaling and the inactivation of Bad.

It is thought that iron-induced cardiac injury is initiated, at least partially, by the generation of reactive hydroxyl radicals (HO) which if excessive can damage cellular macromolecules and lead to the initiation of cellular apoptosis (Ambrosio et al., 1987; Bolli et al., 1987; Ambrosio et al., 1998). In vitro models which have examined the effects of elevated iron have shown that increased iron initially causes an elevation of Akt phosphorylation however this effect appears to be reversed following prolonged exposure (Kuperstein and Yavin, 2003; Chen et al., 2007). Why this shift from an anti-apoptotic-state (i.e. increased Akt phosphorylation) to one that is more permissive to apoptosis (i.e. diminished Akt phosphorylation) occurs is not well understood but may be related to chronic elevations in the amount of iron-associated reactive oxygen species (ROS). Supporting this contention, recent data from our laboratory has demonstrated that persistent elevations in oxidative stress, such as that seen during the aging process, are associated with the post-translational modification (S-nitrosylation) of Akt, impairments in Akt enzymatic function and its downstream effectors (Wu et al., 2009b; Wu et al., 2010a; Wu et al., 2010b). In the current study, we observe reduced Akt activation with iron overload and demonstrate that this finding is reversed by iron chelation. Whether combination based therapies aimed at decreasing tissue iron levels while also diminishing oxidative stress, perhaps through the concomitant administration of ROS scavengers, may lead to further beneficial effects will require further study. However it is interesting to note that the administration of deferoxamine along with acetaminophen (a potent antioxidant) has demonstrated a greater capacity to remove cardiac iron in the iron-overloaded gerbil (Walker et al., 2009).

In summary, our data demonstrate that deferasirox treatment is associated with reduced cardiac fibrosis following iron overload. This effect is accompanied by a reduction of apoptosis, a finding that is related to a reduced cleavage of alpha-fodrin, improvements in cell membrane integrity and decreased nucleic DNA fragmentation. These alterations appears to arise from deferasirox associated decreases in

capase-3 activation that may be mediated by reduction in pro-apoptotic Bax / Bcl-2 ratio and increased phosphorylation (inhibition) of Bad via Akt activation (Figure 6). The findings of this study provide insight regarding the potential utility of deferasirox treatment for attenuating iron-induced cardiac tissue damage.

Authorship Contributions:

Participated in research design: Miaozong Wu and Eric R. Blough.

Conducted experiments: Yeling Wang, Miaozong Wu, Rabaa Al-Rousan, Hua Liu, Jacqueline Fannin, Satyanarayana Paturi, Ravi Kumar Arvapalli, Anjaiah Katta, Sunil K. Kakarla, Kevin M. Rice, and William E. Triest.

Performed data analysis: Miaozong Wu and Yeling Wang.

Wrote or contributed to the writing of the manuscript: Miaozong Wu, Yeling Wang, and Eric R. Blough.

Other: Eric R. Blough acquired funding for the research.

References

Abetz L, Baladi JF, Jones P and Rofail D (2006) The impact of iron overload and its treatment on quality of life: results from a literature review. *Health Qual Life Outcomes* **4**:73.

Al-Rousan RM, Paturi S, Laurino JP, Kakarla SK, Gutta AK, Walker EM and Blough ER (2009) Deferasirox removes cardiac iron and attenuates oxidative stress in the iron-overloaded gerbil. *Am J Hematol* **84**:565-570.

Ambrosio G, Zweier JL and Becker LC (1998) Apoptosis is prevented by administration of superoxide dismutase in dogs with reperfused myocardial infarction. *Basic Res Cardiol* **93**:94-96.

Ambrosio G, Zweier JL, Jacobus WE, Weisfeldt ML and Flaherty JT (1987) Improvement of postischemic myocardial function and metabolism induced by administration of deferoxamine at the time of reflow: the role of iron in the pathogenesis of reperfusion injury. *Circulation* **76**:906-915.

Arvapalli RK, Paturi S, Laurino JP, Katta A, Kakarla SK, Gadde MK, Wu M, Rice KM, Walker EM, Wehner P and Blough ER (2010) Deferasirox decreases age-associated iron accumulation in the aging F344XBN rat heart and liver. *Cardiovasc Toxicol* **10**:108-116.

Bolli R, Patel BS, Zhu WX, O'Neill PG, Hartley CJ, Charlat ML and Roberts R (1987) The iron chelator desferrioxamine attenuates postischemic ventricular dysfunction. *Am J Physiol* **253**:H1372-1380.

Borgna-Pignatti C, Cappellini MD, De Stefano P, Del Vecchio GC, Forni GL, Gamberini MR, Ghilardi R, Origa R, Piga A, Romeo MA, Zhao H and Cnaan A (2005) Survival and complications in thalassemia. *Ann N Y Acad Sci* **1054**:40-47.

Burke W, Reyes M and Imperatore G (2002) Hereditary haemochromatosis: a realistic approach to prevention of iron overload disease in the population. *Best Pract Res Clin Haematol* **15**:315-328.

Burlew BS and Weber KT (2002) Cardiac fibrosis as a cause of diastolic dysfunction. *Herz* **27**:92-98.

Carlini RG, Alonzo E, Bellorin-Font E and Weisinger JR (2006) Apoptotic stress pathway activation mediated by iron on endothelial cells in vitro. *Nephrol Dial Transplant* **21**:3055-3061.

Chen L, Xiong S, She H, Lin SW, Wang J and Tsukamoto H (2007) Iron causes interactions of TAK1, p21ras, and phosphatidylinositol 3-kinase in caveolae to activate IkappaB kinase in hepatic macrophages. *J Biol Chem* **282**:5582-5588.

Datta SR, Dudek H, Tao X, Masters S, Fu H, Gotoh Y and Greenberg ME (1997) Akt phosphorylation of BAD couples survival signals to the cell-intrinsic death machinery. *Cell* **91**:231-241.

Dolber PC and Spach MS (1987) Picrosirius red staining of cardiac muscle following phosphomolybdic acid treatment. *Stain Technol* **62**:23-26.

Ervasti JM and Campbell KP (1993) A role for the dystrophin-glycoprotein complex as a transmembrane linker between laminin and actin. *J Cell Biol* **122**:809-823.

Fadeel B (2004) Plasma membrane alterations during apoptosis: role in corpse clearance. *Antioxid Redox Signal* **6**:269-275.

Gross A, Jockel J, Wei MC and Korsmeyer SJ (1998) Enforced dimerization of BAX results in its translocation, mitochondrial dysfunction and apoptosis. *Embo J* **17**:3878-3885.

Gurtl B, Kratky D, Guelly C, Zhang L, Gorkiewicz G, Das SK, Tamilarasan KP and Hoefler G (2009) Apoptosis and fibrosis are early features of heart failure in an animal model of metabolic cardiomyopathy. *Int J Exp Pathol* **90**:338-346.

Janicke RU, Ng P, Sprengart ML and Porter AG (1998) Caspase-3 is required for alpha-fodrin cleavage but dispensable for cleavage of other death substrates in apoptosis. *J Biol Chem* **273**:15540-15545.

Kakarla SK, Fannin JC, Keshavarzian S, Katta A, Paturi S, Nalabotu SK, Wu M, Rice KM, Manzoor K, Walker EM, Jr. and Blough ER (2010) Chronic acetaminophen attenuates age-associated increases in cardiac ROS and apoptosis in the Fischer Brown Norway rat. *Basic Res Cardiol* **105**:535-544.

Kohgo Y, Ikuta K, Ohtake T, Torimoto Y and Kato J (2008) Body iron metabolism and pathophysiology of iron overload. *Int J Hematol* **88**:7-15.

Kooncumchoo P, Sharma S, Porter J, Govitrapong P and Ebadi M (2006) Coenzyme Q(10) provides neuroprotection in iron-induced apoptosis in dopaminergic neurons. *J Mol Neurosci* **28**:125-141.

Korsmeyer SJ, Shutter JR, Veis DJ, Merry DE and Oltvai ZN (1993) Bcl-2/Bax: a rheostat that regulates an anti-oxidant pathway and cell death. *Semin Cancer Biol* **4**:327-332.

Kuperstein F and Yavin E (2003) Pro-apoptotic signaling in neuronal cells following iron and amyloid beta peptide neurotoxicity. *J Neurochem* **86**:114-125.

Majno G and Joris I (1995) Apoptosis, oncosis, and necrosis. An overview of cell death. *Am J Pathol* **146**:3-15.

Martin SJ, O'Brien GA, Nishioka WK, McGahon AJ, Mahboubi A, Saido TC and Green DR (1995) Proteolysis of fodrin (non-erythroid spectrin) during apoptosis. *J Biol Chem* **270**:6425-6428.

Murphy KM, Ranganathan V, Farnsworth ML, Kavallaris M and Lock RB (2000) Bcl-2 inhibits Bax translocation from cytosol to mitochondria during drug-induced apoptosis of human tumor cells. *Cell Death Differ* **7**:102-111.

Narita M, Shimizu S, Ito T, Chittenden T, Lutz RJ, Matsuda H and Tsujimoto Y (1998) Bax interacts with the permeability transition pore to induce permeability transition and cytochrome c release in isolated mitochondria. *Proc Natl Acad Sci U S A* **95**:14681-14686.

Neufeld EJ (2006) Oral chelators deferasirox and deferiprone for transfusional iron overload in thalassemia major: new data, new questions. *Blood* **107**:3436-3441.

Oudit GY, Trivieri MG, Khaper N, Husain T, Wilson GJ, Liu P, Sole MJ and Backx PH (2004) Taurine supplementation reduces oxidative stress and improves cardiovascular function in an iron-overload murine model. *Circulation* **109**:1877-1885.

Pennell DJ, Porter JB, Cappellini MD, El-Beshlawy A, Chan LL, Aydinok Y, Elalfy MS, Sutcharitchan P, Li CK, Ibrahim H, Viprakasit V, Kattamis A, Smith G, Habr D, Domokos G, Roubert B and Taher A (2010) Efficacy of deferasirox in reducing and preventing cardiac iron overload in beta-thalassemia. *Blood* **115**:2364-2371.

Porter AG and Janicke RU (1999) Emerging roles of caspase-3 in apoptosis. *Cell Death Differ* **6**:99-104.

Takada Y, Hashimoto M, Kasahara J, Aihara K and Fukunaga K (2004) Cytoprotective effect of sodium orthovanadate on ischemia/reperfusion-induced injury in the rat heart involves Akt activation and inhibition of fodrin breakdown and apoptosis. *J Pharmacol Exp Ther* **311**:1249-1255.

Walker EM, Jr., Morrison RG, Dornon L, Laurino JP, Walker SM, Studeny M, Wehner PS, Rice KM, Wu M and Blough ER (2009) Acetaminophen combinations protect against iron-induced cardiac damage in gerbils. *Ann Clin Lab Sci* **39**:378-385.

Whittaker P, Hines FA, Robl MG and Dunkel VC (1996) Histopathological evaluation of liver, pancreas, spleen, and heart from iron-overloaded Sprague-Dawley rats. *Toxicol Pathol* **24**:558-563.

Wu M, Desai DH, Kakarla SK, Katta A, Paturi S, Gutta AK, Rice KM, Walker EM, Jr. and Blough ER (2009a) Acetaminophen prevents aging-associated hyperglycemia in aged rats: effect of aging-associated hyperactivation of p38-MAPK and ERK1/2. *Diabetes Metab Res Rev* **25**:279-286.

Wu M, Falasca M and Blough ER (2010a) Akt / protein kinase B in skeletal muscle physiology and pathology. *J Cell Physiol*: in press.

Wu M, Katta A, Gadde MK, Liu H, Kakarla SK, Fannin J, Paturi S, Arvapalli RK, Rice KM, Wang Y and Blough ER (2009b) Aging-associated dysfunction of akt/protein kinase B: s-nitrosylation and acetaminophen intervention. *PLoS One* **4**:e6430.

Wu M, Liu H, Fannin J, Katta A, Wang Y, Arvapalli RK, Paturi S, Karkala SK, Rice KM and Blough ER (2010b) Acetaminophen Improves Protein Translational Signaling in Aged Skeletal Muscle. *Rejuvenation Res*: in press.

Wu M, Wang B, Fei J, Santanam N and Blough ER (2010c) Important roles of Akt/PKB signaling in the aging process. *Front Biosci (Schol Ed)* **2**:1169-1188.

Yang E, Zha J, Jockel J, Boise LH, Thompson CB and Korsmeyer SJ (1995) Bad, a heterodimeric partner for Bcl-XL and Bcl-2, displaces Bax and promotes cell death. *Cell* **80**:285-291.

Zha J, Harada H, Yang E, Jockel J and Korsmeyer SJ (1996) Serine phosphorylation of death agonist BAD in response to survival factor results in binding to 14-3-3 not BCL-X(L). *Cell* **87**:619-628.

Zhang JH and Xu M (2000) DNA fragmentation in apoptosis. *Cell Res* **10**:205-211.

Footnotes:

This work was supported by funding provided by Novartis Pharmaceutical to E.R.B.

Wang Y. and Wu M. contributed equally to this work.

Figure legends

Figure 1. Deferasirox treatment reduces cardiac iron deposition and iron overload-induced changes in ferritin protein expression. **A**. Representative images of heart sections reacted with Perl's iron stain from adult male Mongolian gerbils that had been subjected to iron overload for 10 weeks (IO), iron overloaded and then treated with deferasirox for 3 months (IO-DFR), or iron overloaded and treated with vehicle (peanut butter; IO-3m). The symbols (C) and (C-3m) represent age-matched controls for the 10-week iron loading protocol (C) and age-matched control for the 3-month treated animals (C-3m). Arrow indicates iron-deposition (blue). Three hearts from each group and 8-10 randomly-selected areas from each heart were used for quantification of iron. The degree of iron deposition was determined by dividing the area positive for iron by total tissue area. **B**. Expression of cardiac ferritin heavy chain (FHC) and light chain (FLC) proteins were determined by immunoblotting. Data are mean ± SE (n = 4-6). abcd: Groups without the same letter are significantly different ($P < 0.05$).

Figure 2. Deferasirox diminishes iron-induced myocardial fibrosis. Picro-sirius red stain was used to determine collagen deposition in adult male Mongolian gerbils that had been subjected to iron overload for 10 weeks (IO), iron overloaded and then treated with deferasirox for 3 months (IO-DFR) or iron overloaded and treated with vehicle (peanut butter; IO-3m). The symbols (C) and (C-3m) represent age-matched controls for the 10-week iron loading protocol (C) and age-matched control for the 3-month treated animals (C-3m). Arrow indicates an area with elevated collagen deposition (red color). Three hearts from each group and 8-10 randomly-selected areas from each heart were used for quantification of collagen. The degree of collagen deposition was determined by dividing the area positive for collagen by total tissue area. Data are mean ± SE. abc: Groups without the same letter are significantly different ($P < 0.05$).

Figure 3. Deferasirox decreases the number of TUNEL positive cells after iron overload. Representative images of TUNEL-stained nuclei from adult male Mongolian gerbils that had been subjected to iron overload for 10 weeks (IO), iron overloaded and then treated with deferasirox for 3 months (IO-DFR) or iron overloaded and treated with vehicle (peanut butter; IO-3m). The symbols (C) and (C-3m) represent age-matched controls for the 10-week iron loading protocol (C) and age-matched control for the 3-month treated animals (C-3m). Three hearts from each group and 8-10 randomly-selected areas from each heart were used for quantification of TUNEL positive cells. Sections were triple-stained with TUNEL (green, DNA strand breaks), DAPI (blue, nuclei) and dystrophin (Texas red). Arrow indicates examples of TUNEL positive nuclei. Total nuclei counted for C, IO, C-3m, IO-3m and IO-DFR rats were 3545, 3656, 4297, 7807 and 5366, respectively. Apoptotic index is expressed as the number of TUNEL-positive per 100 nuclei (TUNEL+ / 100 nuclei). Data are mean ± SE. abc: Groups without the same letter are significantly different ($P < 0.05$).

Figure 4. Deferasirox decreases iron overload-induced activation of caspases. **A**. The amount of full-length (inactive) and cleaved (active, 19 kDa and 17 kDa fragments) caspase-3 protein in adult Mongolian gerbil cardiac samples was determined via immunoblotting. Animals were subjected to iron overload for 10 weeks (IO), 3 months of deferasirox treatment (IO-DFR) or vehicle treated (IO-3m) after iron overload, age-matched non-iron overload control for the 10-week iron loading protocol (C) and for the 3-month animals (C-3m). There were no difference in the amount of full-length caspase-3 protein between groups ($P = 0.30$). **B**. The abundance of full-length (inactive) and cleaved (active, 40/38 kDa and 17 kDa fragments) caspase-9 protein was determined by immunoblotting. **C**. Full-length (inactive) and cleaved (active, 150- and 120-kDa fragments) cardiac alpha-fodrin levels as quantified by immunoblotting. **D**. Immunohistochemical staining of cardiac sections with dystrophin antibody was used to examine the effects of excess cardiac iron on myocardial membrane integrity. Insert: Magnified image showing myocyte with

discontinuity of dystrophin immunoreactivity following iron overload (arrows). Data are mean± SE (n = 4–6). abc: Groups without the same letter are significantly different (P<0.05).

Figure 5. Deferasirox prevents iron overload–induced alterations in apopotic signaling in the gerbil heart. **A**. Expression of Bax and Bcl-2 were determined using immunoblotting. Animals were subjected to iron overload for 10 weeks (IO), 3 months of deferasirox treatment (IO-DFR) or vehicle treated (IO-3m) after iron overload, age-matched non-iron overload control for the 10-week iron loading protocol (C) and for the 3-month animals (C-3m). There was no difference in the amount of Bax protein abundance between groups (P = 0.10). **B**. Quantification of Bad and Bad phosphorylation (Ser136) as determined by immunoblotting. There were no difference in the amount of Bad protein between groups (P = 0.17). **C**. Measurement of Akt expression and phosphorylation (Ser473 and Thr308) as quantified by immunoblotting. There were no differences in the amount of Akt protein between groups (P = 0.27). Data are mean± SE (n = 4–6). abc: Groups without the same letter are significantly different (P<0.05).

Figure 6. Proposed mechanism(s) of how iron chelation may function to diminish cardiac apoptosis following iron overload. Deferasirox treatment, by decreasing tissue iron, is associated with increases in expression of the anti-apoptotic Bcl-2 and phosphorylation of Akt / Bad, which would favor diminished caspase activation, cellular apoptosis and the initiation of cardiac fibrosis. Green arrow indicates effects of deferasirox treatment (↑ and ↓ represent increase and decrease, respectively).

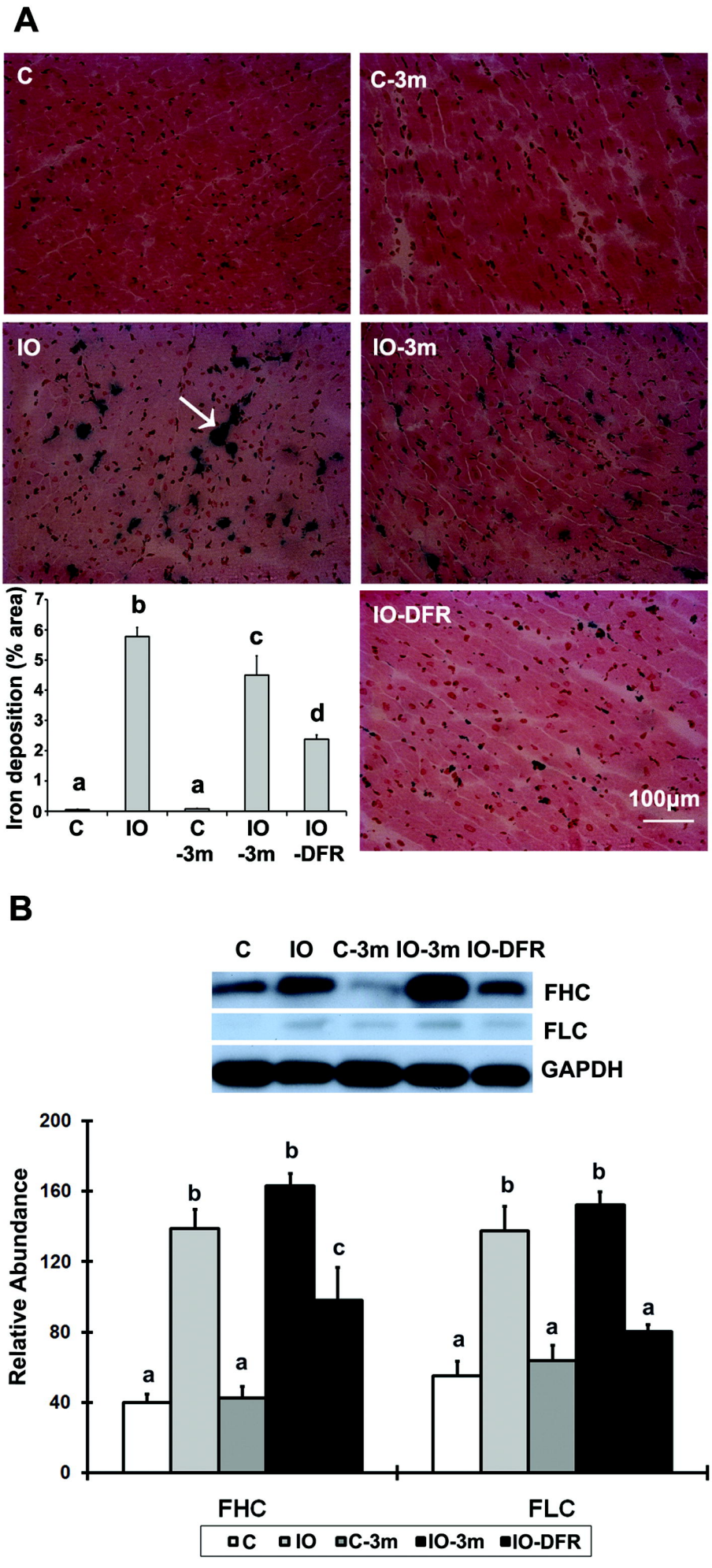
A
C
C-3m
IO
IO-3m
IO-DFR
100μm
Iron deposition (% area)
a
b
a
c
d
C
IO
C -3m
IO -3m
IO -DFR
B
C
IO
C-3m
IO-3m
IO-DFR
FHC
FLC
GAPDH
Relative Abundance
FHC
FLC
C
IO
C-3m
IO-3m
IO-DFR

Figure 1

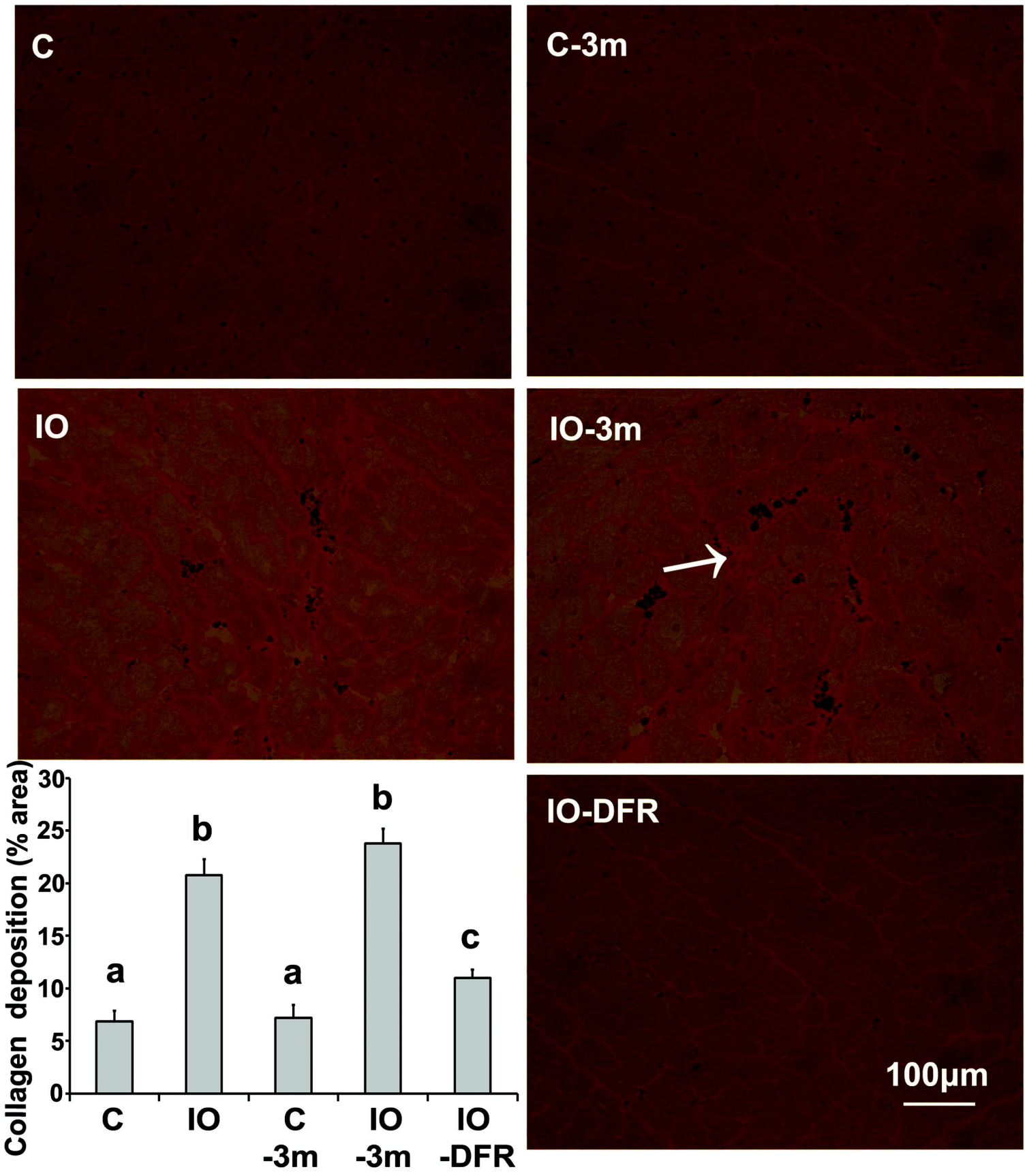
C
C-3m
IO
IO-3m
IO-DFR
100μm
Collagen deposition (% area)
30
25
20
15
10
5
0
a
b
a
b
c
C
IO
C -3m
IO -3m
IO -DFR

Figure 2

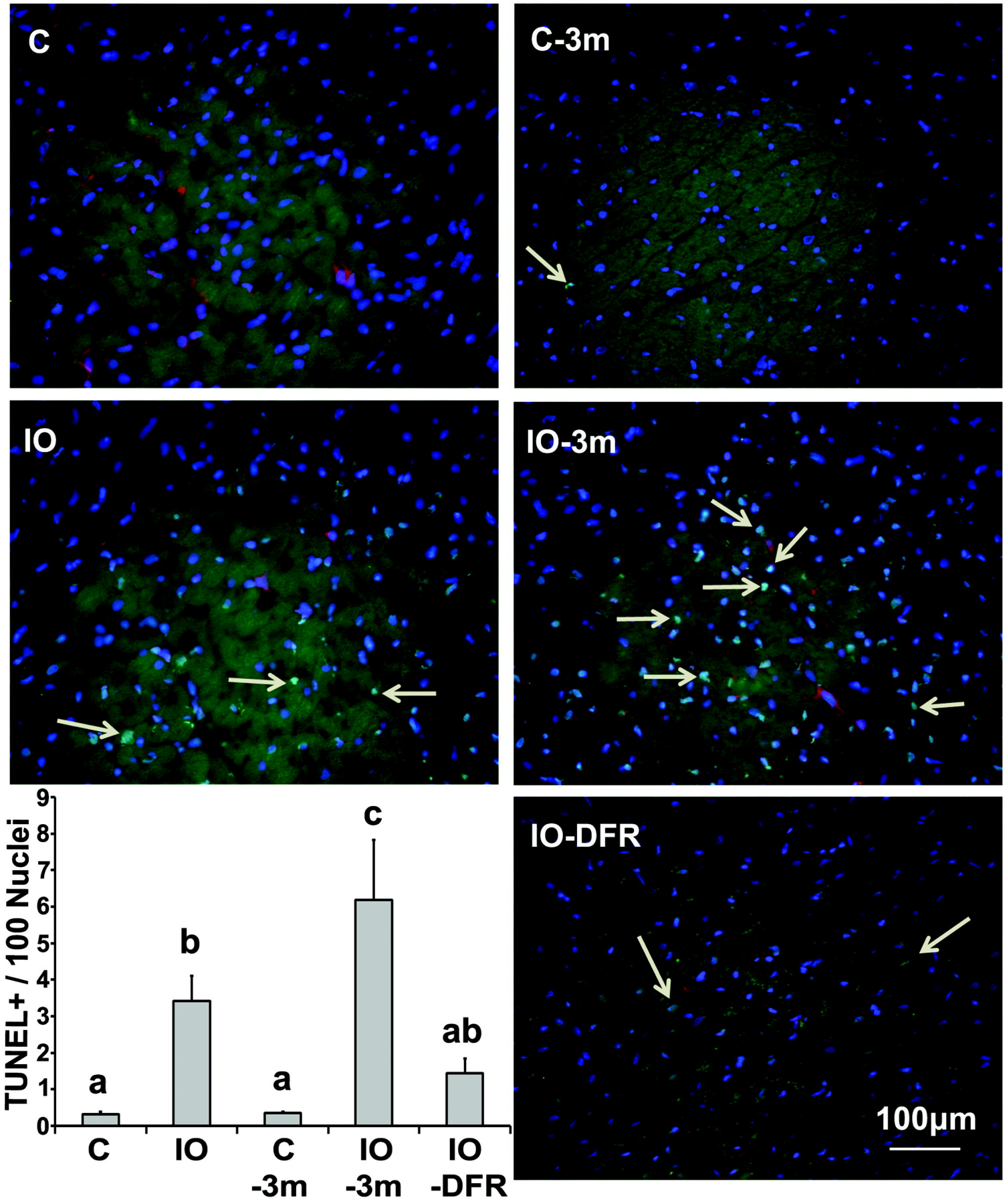
C
C-3m
IO
IO-3m
IO-DFR
100μm
TUNEL+ / 100 Nuclei
0
1
2
3
4
5
6
7
8
9
a
b
a
c
ab
C
IO
C -3m
IO -3m
IO -DFR

Figure 3

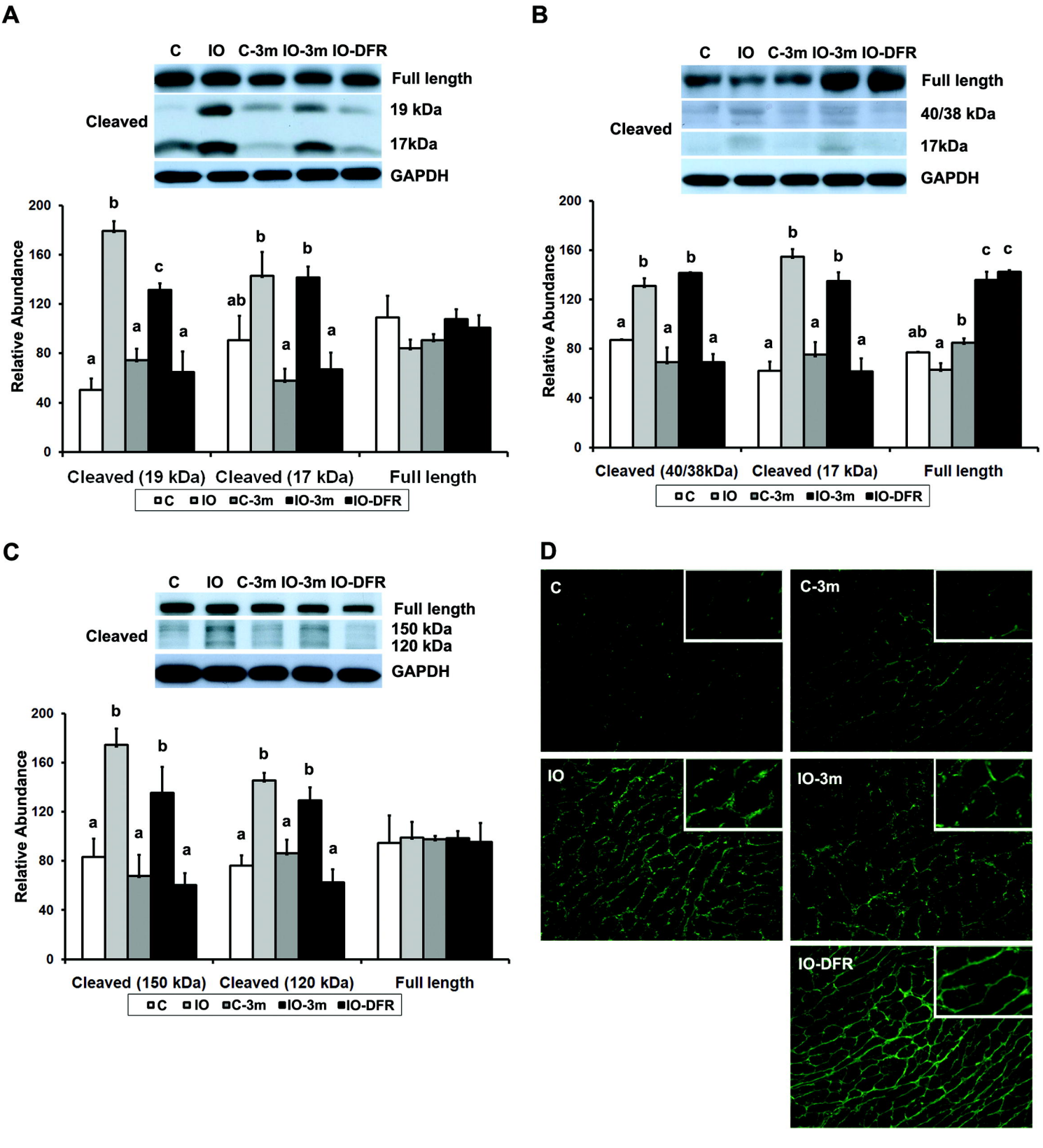
A
C IO C-3m IO-3m IO-DFR
Cleaved
Full length
19 kDa
17kDa
GAPDH
Relative Abundance
Cleaved (19 kDa) Cleaved (17 kDa) Full length
C IO C-3m IO-3m IO-DFR
B
C IO C-3m IO-3m IO-DFR
Cleaved
Full length
40/38 kDa
17kDa
GAPDH
Relative Abundance
Cleaved (40/38kDa) Cleaved (17 kDa) Full length
C IO C-3m IO-3m IO-DFR
C
C IO C-3m IO-3m IO-DFR
Cleaved
Full length
150 kDa
120 kDa
GAPDH
Relative Abundance
Cleaved (150 kDa) Cleaved (120 kDa) Full length
C IO C-3m IO-3m IO-DFR
D
C
C-3m
IO
IO-3m
IO-DFR

Figure 4

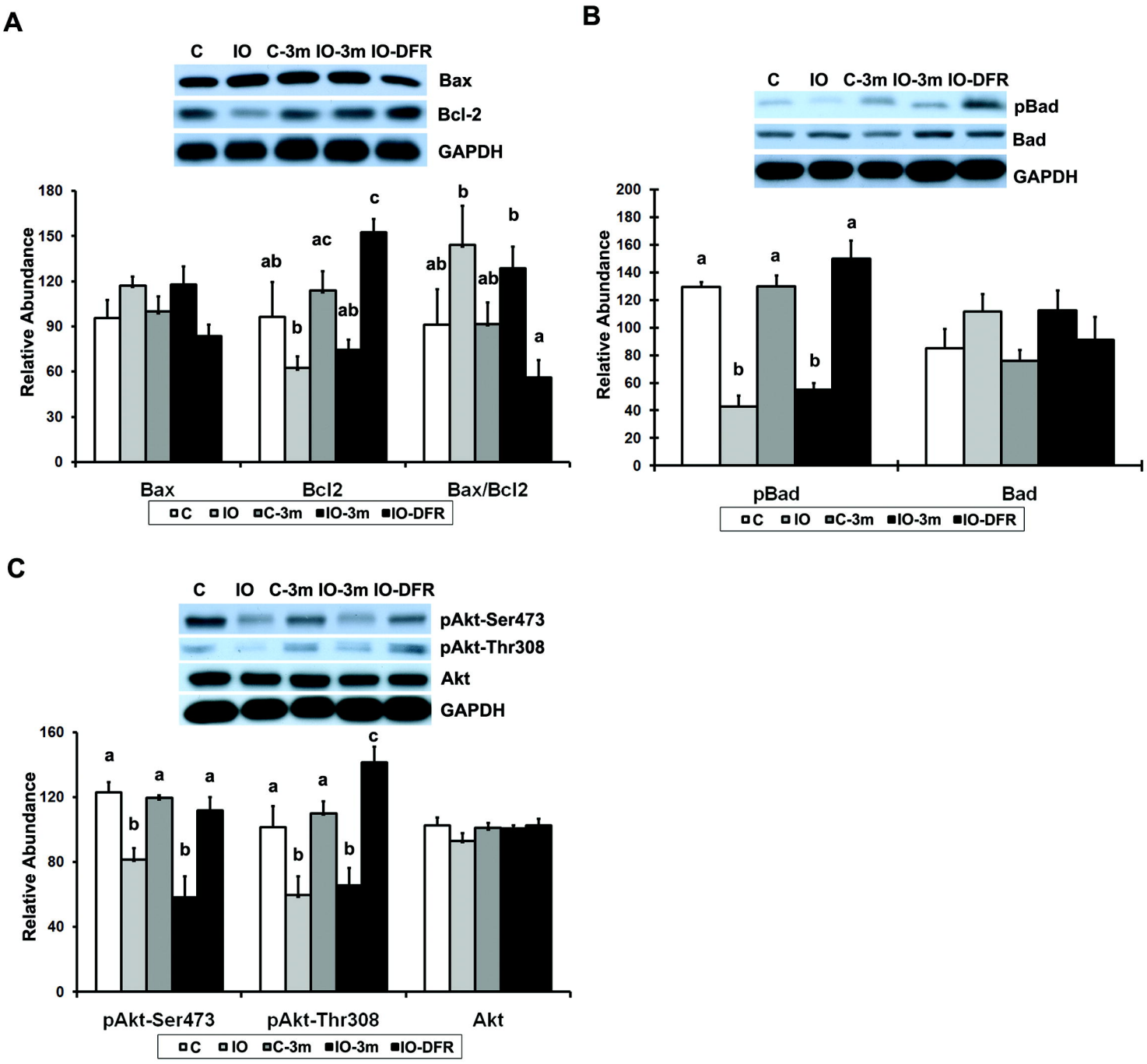
A
C IO C-3m IO-3m IO-DFR
Bax
Bcl-2
GAPDH
Relative Abundance
Bax
Bcl2
Bax/Bcl2
C IO C-3m IO-3m IO-DFR
B
C IO C-3m IO-3m IO-DFR
pBad
Bad
GAPDH
Relative Abundance
pBad
Bad
C IO C-3m IO-3m IO-DFR
C
C IO C-3m IO-3m IO-DFR
pAkt-Ser473
pAkt-Thr308
Akt
GAPDH
Relative Abundance
pAkt-Ser473
pAkt-Thr308
Akt
C IO C-3m IO-3m IO-DFR

Figure 5

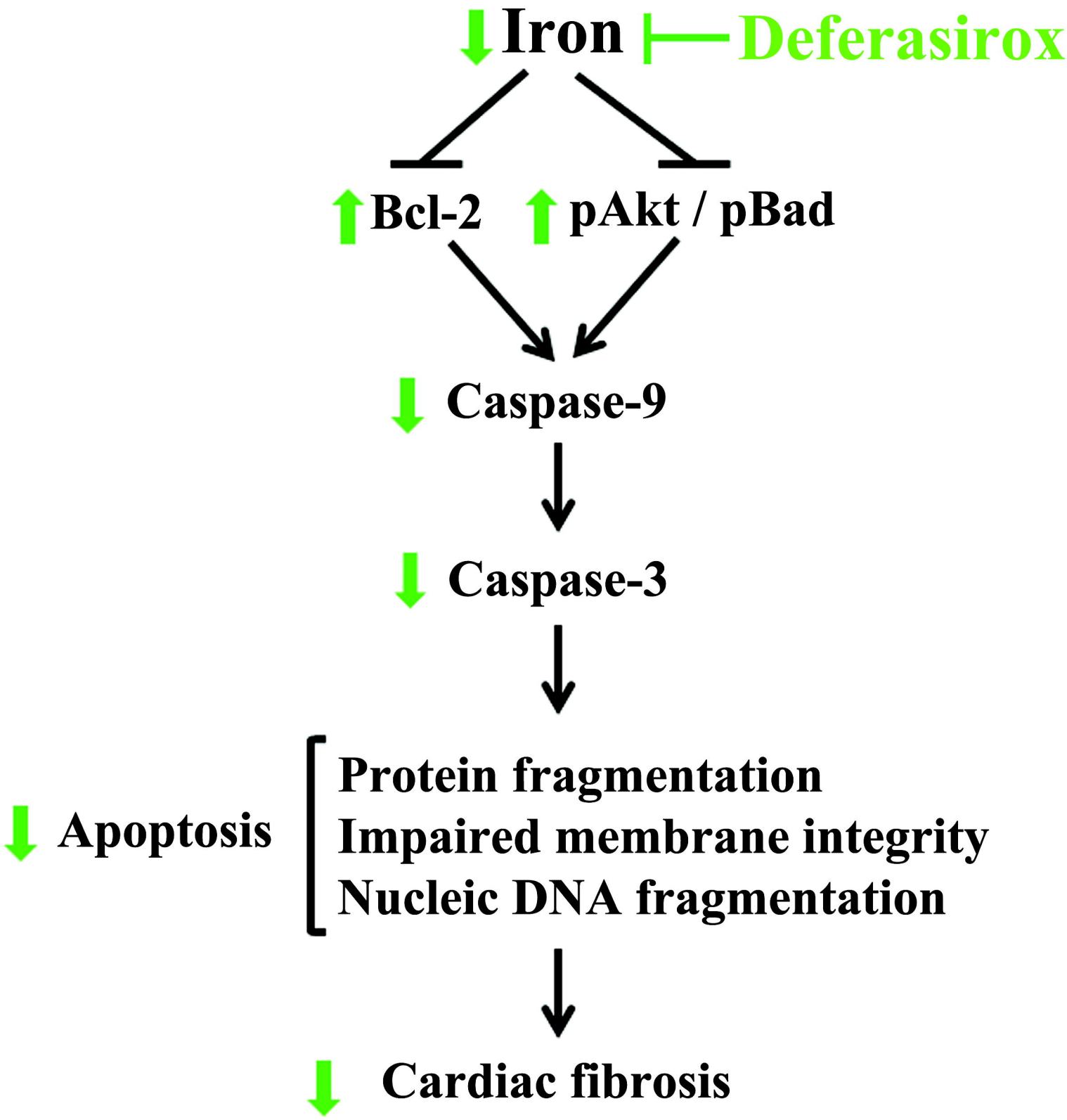
Iron
Deferasirox
Bcl-2
pAkt / pBad
Caspase-9
Caspase-3
Apoptosis
Protein fragmentation
Impaired membrane integrity
Nucleic DNA fragmentation
Cardiac fibrosis

Figure 6